Photoprotection during iron deficiency is mediated by the bHLH transcription factors PYE and ILR3

Garo Z. Akmakjian[a], Nabila Riaz[a], and Mary Lou Guerinot[a,1]

[a]Department of Biological Sciences, Dartmouth College, Hanover, NH 03755

Contributed by Mary Lou Guerinot, August 19, 2021 (sent for review December 18, 2020; reviewed by Bonnie Bartel and Terri A. Long)

Iron (Fe) is an essential micronutrient whose availability is limiting in many soils. During Fe deficiency, plants alter the expression of many genes to increase Fe uptake, distribution, and utilization. In a genetic screen for suppressors of Fe sensitivity in the E3 ligase mutant *bts-3*, we isolated an allele of the bHLH transcription factor (TF) *ILR3*, *ilr3-4*. We identified a striking leaf bleaching phenotype in *ilr3* mutants that was suppressed by limiting light intensity, indicating that ILR3 is required for phototolerance during Fe deficiency. Among its paralogs that are thought to be partially redundant, only *ILR3* was required for phototolerance as well as repression of genes under Fe deficiency. A mutation in the gene-encoding PYE, a known transcriptional repressor under Fe deficiency, also caused leaf bleaching. We identified singlet oxygen as the accumulating reactive oxygen species (ROS) in *ilr3-4* and *pye*, suggesting photosensitivity is due to a PSII defect resulting in ROS production. During Fe deficiency, *ilr3-4* and *pye* chloroplasts retain normal ultrastructure and, unlike wild type (WT), contain stacked grana similar to Fe-sufficient plants. Additionally, we found that the D1 subunit of PSII is destabilized in WT during Fe deficiency but not in *ilr3-4* and *pye*, suggesting that PSII repair is accelerated during Fe deficiency in an ILR3- and PYE-dependent manner. Collectively, our results indicate that ILR3 and PYE confer photoprotection during Fe deficiency to prevent the accumulation of singlet oxygen, potentially by promoting reduction of grana stacking to limit excitation and facilitate repair of the photosynthetic machinery.

Arabidopsis | chloroplasts | iron deficiency | grana | ROS

Iron (Fe) is a critical micronutrient required for most forms of life. Fe deficiency is the most prevalent nutritional disorder in humans and, since most people obtain dietary Fe from plants, it is imperative that we understand how plants sense, obtain, and utilize Fe. In plants, Fe is required for a wide variety of metabolic processes, but Fe is particularly crucial for photosynthesis. Indeed, chloroplasts are the major Fe sink, containing up to 90% of foliar iron (1). Fe acts as a cofactor in both photosystems (2, 3), and Fe deficiency severely limits photosynthetic efficiency (4, 5). It is thus critical that plants acquire sufficient levels of Fe while also adjusting metabolism to compensate for reduced Fe availability and photosynthetic efficiency to optimize Fe utilization and minimize stress (6–8); nutrient economy strategies in general tend to prioritize, recycle, and remobilize limiting nutrients. While Fe uptake by roots has been well studied, the molecular mechanisms underlying adaptations of chloroplasts and photosynthesis during Fe deficiency are not as well understood.

The Fe uptake system is regulated by a transcription factor (TF) cascade that results in the induction of the bHLH transcription factor FER-LIKE FE DEFICIENCY INDUCED TRANSCRIPTION FACTOR (FIT) (also known as bHLH29) (9–11). FIT binds to the promoters of its target genes as a heterodimer with members of the subgroup Ib bHLH transcription factors, bHLH38, bHLH39, bHLH100, and bHLH101 (12, 13). The transcriptional induction of the subgroup Ib bHLH transcription factors depends on the subgroup IVc bHLH transcription factors IAA LEUCINE RESISTANT3 (ILR3) (also known as bHLH105), bHLH115, bHLH34, and bHLH104 (14–16), as well as their more distant paralog, the bHLH subgroup IVb member UPSTREAM REGULATOR OF IRT1 (URI), with which they form heterodimers (17–19). The subgroup IVc bHLH transcription factors also dimerize with another subgroup IVb bHLH transcription factor, POPEYE (PYE) (14, 20), a transcriptional repressor that attenuates the expression of Fe deficiency–induced genes in roots. It has been proposed that PYE and ILR3 repress the expression of *FERRITIN* (*FER*) genes (21); however, it is not known whether all heterodimer pairs among the subgroup IVc transcription factors and PYE are functional or whether they have overlapping functions.

The subgroup IVc bHLH transcription factors are not transcriptionally induced by Fe deficiency (14–16), but instead are regulated posttranslationally by the RING E3 ubiquitin ligase BRUTUS (BTS) (14, 16, 22). Mutations in *BTS* cause constitutive expression of the Fe deficiency response regardless of Fe availability, leading to Fe accumulation and toxicity under Fe-replete conditions and resistance to chlorosis under Fe-depleted conditions, indicating that BTS is a repressor of the Fe deficiency response (14, 23). BTS directly interacts with ILR3, bHLH104, and bHLH115 (20, 22), suggesting that they are potential downstream ubiquitination targets of BTS. This hypothesis is supported by the ability of *ilr3*, *bhlh104*, and *bhlh115* mutants to suppress *bts* mutant phenotypes (14, 16, 24). This indicates that BTS acts upstream of the Fe deficiency transcriptional network in roots, possibly by targeting the subgroup IVc bHLH transcription factors for degradation in Fe-sufficient plants.

In contrast to our understanding of the Fe deficiency response in roots, little is known about the regulation of the Fe deficiency response in leaves. The transcription factor FIT is expressed solely in roots (9–11) and thus is not expected to regulate gene expression in shoots. Conversely, the subgroup Ib bHLH transcription

Significance

Iron deficiency has many adverse effects on photosynthesis, which is not surprising given that 90% of foliar iron is found in the chloroplast. Although many iron-sparing mechanisms have been documented, a mechanistic understanding of how chloroplasts adapt to iron deficiency was lacking. Here, we show that the bHLH transcription factors ILR3 and PYE are required for photoprotection during iron deficiency. Changes in chloroplast morphology under the control of these transcription factors prevents the production of harmful reactive oxygen species and allows for repair of photosystem II. Understanding how plants adapt the photosynthetic machinery during iron deficiency may allow us to optimize plant growth in soils where iron is not bioavailable.

Author contributions: G.Z.A., N.R., and M.L.G. designed research; G.Z.A. and N.R. performed research; G.Z.A., N.R., and M.L.G. analyzed data; and G.Z.A., N.R., and M.L.G. wrote the paper.

Reviewers: B.B., Rice University; T.A.L., North Carolina State University

The authors declare no competing interest.

[1]To whom correspondence may be addressed. Email: Guerinot@Dartmouth.edu.

This article contains supporting information online at https://www.pnas.org/lookup/suppl/doi:10.1073/pnas.2024918118/-/DCSupplemental.

Published September 27, 2021.

factors are expressed in both roots and shoots (25); however, transcriptomic analysis of *bhlh100 bhlh101* double mutants revealed no misregulation of Fe-regulated genes in shoots compared to WT plants (26), possibly due to the redundancy among the subgroup Ib bHLH transcription factors (13). The role of the subgroup IVc bHLH transcription factors, PYE and URI in the shoots has not been investigated. We thus lack data on how Fe deficiency–responsive genes in the shoot are regulated.

Fe deficiency has a profound impact on photosynthesis and chloroplast biology, including loss of photosynthetic efficiency (5, 27–29), remodeling of the photosynthetic apparatus (30, 31), differential changes in Fe-dependent chloroplast proteins (6), and ultrastructural changes of internal membranes, particularly reduction in grana stacking, which has been reported in many species, including barley (32), sugar beet (4), and rice (33). The mechanisms by which plants adapt to Fe deficiency–induced alterations of photosynthesis, however, are not clear. Furthermore, as changes in gene expression and protein accumulation of Fe-dependent proteins can reflect a rebalancing of the Fe economy (6, 7), it remains unknown whether observed physiological changes in chloroplast function during Fe deficiency are due to a physiological response to cope with Fe deficiency or a direct consequence of Fe depletion in the chloroplast.

In a screen to identify genetic suppressors of *bts-3*, we isolated a mutant allele of *ILR3*, *ilr3-4*. The *ilr3-4* mutation suppressed the Fe sensitivity phenotype as well as the constitutive up-regulation of Fe uptake genes in *bts-3*, indicating that ILR3 is an activator of the Fe deficiency response acting downstream of BTS. We found that *ILR3* is critical for regulating Fe deficiency–responsive genes in shoots. Gene misregulation in *ilr3-4* mutants resulted in severe leaf bleaching during Fe deficiency that was suppressed by limiting light exposure, indicating that *ILR3* is required for photoprotection during Fe deficiency. The paralogs of *ILR3* (*bHLH34*, *bHLH104*, and *bHLH115*), in contrast, are not required for photoprotection. We also found that *pye* mutants bleach in a light-dependent manner, suggesting that ILR3 and PYE may act together to protect against light stress. We identified singlet oxygen as the reactive oxygen species (ROS) that accumulates in Fe-deficient *ilr3* and *pye*, suggesting that PSII is the major target of damage to chloroplasts during Fe deficiency. Interestingly, while grana destack during Fe deficiency in WT plants, grana remain intact in Fe-deficient *ilr3-4* and *pye* mutant plants, accompanied by decreased D1 protein turnover and thus lower PSII repair. We thus propose that ILR3 and PYE mediate grana destacking to accelerate the rate of PSII repair, mitigating the production of singlet oxygen during Fe deficiency.

Results

***ILR3* Is a Genetic Suppressor of *bts-3*.** BTS is a repressor of Fe uptake genes in the roots, and the *bts-3* mutant thus constitutively expresses Fe uptake genes in the presence of Fe (14, 23). Consequently, *bts-3* mutants overaccumulate Fe and grow poorly under Fe-sufficient conditions. We leveraged this severe growth phenotype and performed a genetic screen to identify suppressors of the Fe sensitivity phenotype in *bts-3* mutants. We screened ethyl methanesulfonate (EMS)-mutagenized *bts-3* plants on Fe-ethylenediamine-N,N′-bis(2-hydroxyphenylacetic acid) (Fe-EDDHA) fertilized soil and isolated a suppressor mutant. When grown on Fe-replete medium, *bts-3* mutants showed stunted growth (Fig. 1*A*). The suppressor mutant, however, did not exhibit this Fe sensitivity and grew similarly to wild-type (WT) plants under Fe-replete conditions (Fig. 1*A*). We isolated the single mutant carrying the suppressing mutation and found that the single mutant also grew similarly to WT plants under Fe-sufficient conditions. After transferring plants to Fe-deficient medium, growth of *bts-3* mutants was rescued and *bts-3* mutants were less chlorotic than WT (Fig. 1*A*). The Fe deficiency resistance in *bts-3* mutants was also suppressed and single and double mutants carrying the suppressing mutation grew very poorly and developed

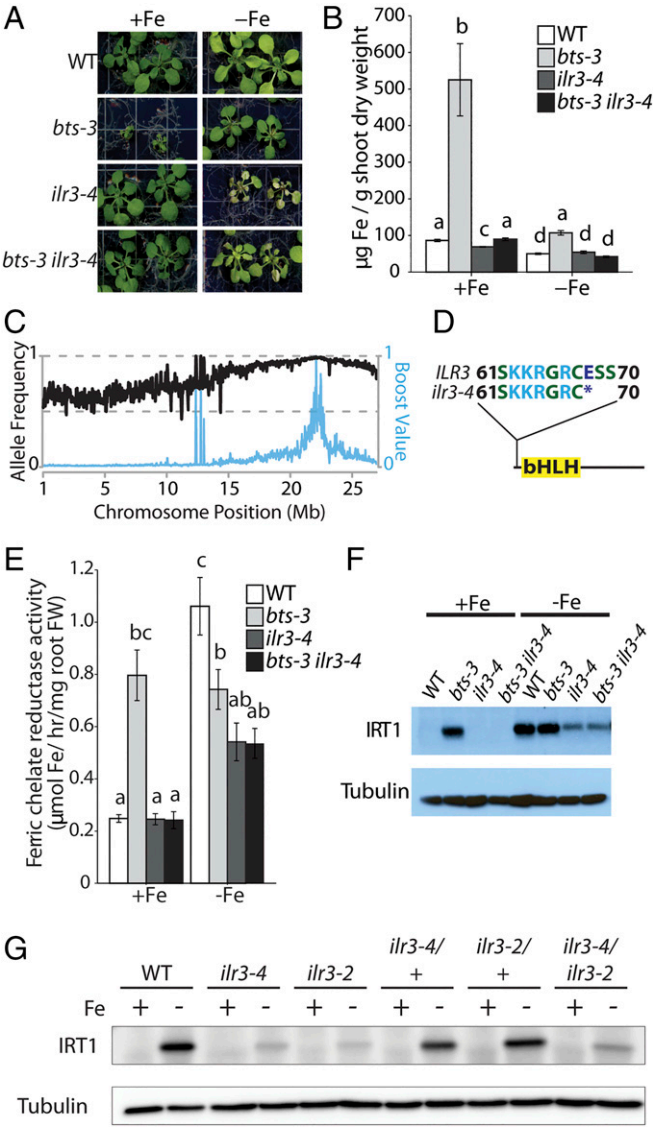

Fig. 1. *ilr3-4* is a suppressor of *bts-3*. (*A*) *ilr3-4* suppresses sensitivity to high Fe and tolerance to Fe deficiency. Plants grown on 1/2 strength B5 medium for 2 wk were transferred to Fe-sufficient or Fe-deficient media for 6 d. (*B*) *ilr3-4* suppresses Fe overaccumulation. Plants grown on 1/2 strength B5 medium for 2 wk were transferred to Fe-sufficient or Fe-deficient media for 5 d. Shoots were harvested for metal quantification by ICP-MS ($n = 4$). Different letters indicate $P < 0.05$ by Tukey's test. (*C*) SHOREmap output of chromosome 5 from a *bts-3 ilr3-4* × Ler-0 outcross. The black line represents the frequency of the WT single nucleotide polymorphism (SNP) allele and the blue line represents the estimated mapping interval determined by the boost value (34). (*D*) Schematic representation of ILR3 and indication of the mutation in *ilr3-4*. (*E*) *ilr3-4* suppresses Fe chelate reductase activity in *bts-3* roots for plants grown in Fe-sufficient conditions. Fe chelate reductase activity was determined in plants grown on 1/2 strength B5 medium for 2 wk and transferred to Fe-sufficient or Fe-deficient media for 3 d ($n = 8$). Different letters indicate $P < 0.05$ by Tukey's test. (*F*) *ilr3-4* suppresses the high IRT1 protein levels in *bts-3* roots for plants grown in Fe-sufficient conditions. Western blotting against IRT1 was performed on total root protein extracted from plants grown on 1/2 strength B5 medium for 2 wk and transferred to Fe-sufficient or Fe-deficient media for 3 d. α-Tubulin is shown as a loading control. (*G*) *ilr3-2* and *ilr3-4* are allelic. WT, *ilr3-4*, *ilr3-2*, *ilr3-4*/+, *ilr3-2*/+, and *ilr3-4*/*ilr3-2* plants grown for 2 wk on 1/2 strength B5 medium were transferred to Fe-sufficient or Fe-deficient media for 3 d. Western blotting was performed against IRT1. α-Tubulin is shown as a loading control.

bleached leaves under Fe-deficient conditions (Fig. 1*A*). Inductively coupled plasma-mass spectrometry (ICP-MS) analysis of shoots confirmed that the suppressing mutation ameliorated Fe overaccumulation in *bts-3* mutants under Fe-sufficient conditions (Fig. 1*B*). While the single mutant had a slightly lower foliar Fe concentration than WT under Fe-sufficient conditions, Fe levels were similar among WT, the single mutant, and the double mutant plants under Fe-deficient conditions but higher in *bts-3* mutants (Fig. 1*B*).

To identify the causative mutation, the double mutant was outcrossed to L*er*-0. The F_2 population was screened under Fe deficiency and plants exhibiting bleached leaves were selected and pooled for whole-genomic resequencing. Using SHOREmap (34), we narrowed down a mapping interval on chromosome 5 (Fig. 1*C*). We identified a premature stop codon in the *ILR3* gene at glutamate 68, just upstream of the DNA binding bHLH domain (Fig. 1*D*), which would result in a truncated protein that we would expect to be nonfunctional. This allele is designated *ilr3-4*.

Due to the reduced Fe content in *bts-3 ilr3-4* double mutants compared to *bts-3*, we examined whether *ILR3* is required for Fe reduction mediated by the Fe chelate reductase FERRIC REDUCTASE OXIDASE2 (FRO2) and expression of the high-affinity iron transporter IRON REGULATED TRANSPORTER1 (IRT1), both of which are induced during the Fe deficiency response (34, 35). Fe chelate reductase activity was elevated in *bts-3* compared to WT plants under Fe-sufficient conditions (Fig. 1*E*). Similarly, IRT1 protein accumulated in *bts-3* regardless of Fe availability, whereas IRT1 was only detectable in WT plants during Fe deficiency, consistent with the role of BTS as a repressor of Fe uptake (Fig. 1*F*). The accumulation of IRT1 protein and high Fe chelate reductase activity of *bts-3* mutants grown in Fe-sufficient medium was suppressed by the *ilr3-4* mutation (Fig. 1 *E* and *F*). Additionally, the *bts-3 ilr3-4* and *ilr3-4* mutants were impaired in the induction of IRT1 protein levels and had lower Fe chelate reductase activity than WT plants during Fe deficiency, confirming that *ILR3* is required for full induction of IRT1 expression and Fe chelate reductase activity during Fe deficiency in WT plants and in Fe-sufficient *bts-3* mutants.

To prove that *ilr3-4* was indeed an allele of *ILR3*, we obtained the T-DNA null allele *ilr3-2* and carried out genetic complementation. If two recessive mutations are allelic, they fail to complement in the F_1 hybrids. We used IRT1 protein induction as a readout of whether the transheterozygote behaved like a loss-of-function mutant. While heterozygous lines for either *ilr3-2* and *ilr3-4* exhibited IRT1 protein induction, the *ilr3-2*/*ilr3-4* transheterozygote showed defective IRT1 protein induction similar to plants homozygous for either mutant allele (Fig. 1*G*), confirming that the phenotype in *ilr3-4* is due to the mutation in *ILR3*.

At the transcriptional level, constitutive expression of *IRT1* and *FRO2* in *bts-3* mutants was suppressed in *bts-3 ilr3-4* mutants and the expression of *IRT1* and *FRO2* during Fe deficiency was lower in *ilr3-4* compared to WT (Fig. 2), consistent with reduced IRT1 protein levels and ferric chelate reductase activity in this mutant (Fig. 1 *E* and *F*). We also measured the expression of the transcriptional activators of IRT1 and FRO2, FIT, bHLH38, bHLH39, bHLH100, and bHLH101. The *ilr3-4* mutation suppressed the high expression of all these transcription factors in *bts-3* when grown under Fe-sufficient conditions (Fig. 2). Under Fe-deficient conditions, the expression of Fe-regulated transcription factors was strongly reduced in *ilr3-4* compared to WT plants (Fig. 2) as previously reported for *ilr3-2* (14). Furthermore, the expression of bHLH38, bHLH39, and FIT was also reduced in *bts-3 ilr3-4* mutants during Fe deficiency compared to WT plants, confirming that ILR3 functions upstream of the subgroup Ib bHLH transcription factors to induce their expression during Fe deficiency.

***ILR3* Is Necessary for Photoprotection during Fe Deficiency.** When grown on Fe-sufficient medium, *ilr3-4* mutants grew similarly to WT plants and did not exhibit any symptoms of Fe deficiency

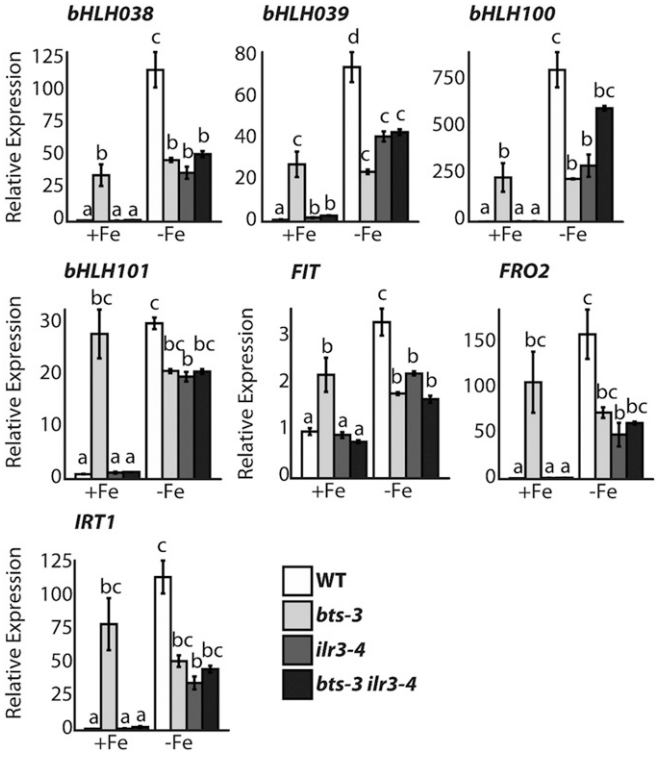

Fig. 2. ILR3 is required for full transcriptional induction of the Fe deficiency response in roots. Steady-state transcript levels of *bHLH38*, *bHLH39*, *bHLH100*, *bHLH101*, *FIT*, *IRT1*, and *FRO2* in roots were quantified via real-time qRT-PCR using RNA from plants grown on 1/2 strength B5 medium for 2 wk and transferred to Fe-sufficient or Fe-deficient media for 3 d ($n = 3$). Different letters indicate $P < 0.05$ by Tukey's test.

such as chlorosis (Fig. 3*A*). When transferred to Fe-deficient medium for 6 d, however, we observed a striking difference between the leaves of WT and *ilr3-4* mutants. While WT developed chlorosis as expected, the growth of *ilr3-4* mutants was stunted and *ilr3-4* mutant leaves developed severe interveinal leaf bleaching (Fig. 3 *A* and *B*). Bleaching was also observed in Fe-deficient *ilr3-2* mutants and *ilr3-4*/*ilr3-2* transheterozygotes, but not in *ilr3-4*/+ or *ilr3-2*/+ heterozygotes, verifying that leaf bleaching during Fe deficiency was due to loss of *ILR3*.

Because *ilr3* mutants are unable to fully induce *IRT1* expression, it is possible that leaf bleaching is due to reduced Fe uptake during Fe deficiency in *ilr3-2* and *ilr3-4* compared to WT. To test this hypothesis, we compared the growth of *ilr3-2* and *ilr3-4* under Fe deficiency to *fit-2*, which is unable to express the high-affinity Fe uptake system. Unlike *ilr3-2* and *ilr3-4*, *fit-2* mutants developed chlorosis without any indications of bleaching (Fig. 3*C*). Chlorophyll concentration did not differ between WT and *ilr3-4* but was lower in *fit-2* mutants (*SI Appendix*, Fig. S1*A*). However, intensity distributions from profile scans across the leaves of Fe-deficient leaves highlighted that while *fit-2* leaves are less pigmented than WT leaves, there is a significantly broader range in pigmentation across *ilr3-4* leaves (*SI Appendix*, Fig. S1*C*), indicating that some regions of the leaf are more depigmented than others. This result, in addition to the observation that *ilr3-4* mutants accumulate foliar Fe levels similar to WT, indicates that the leaf bleaching in the *ilr3* mutants is not due solely to misregulation of Fe uptake genes in the roots.

Leaf bleaching is a phenotype commonly observed during high-light stress (36). Because chloroplasts are the major sink for foliar Fe (1) and photosynthesis is strongly perturbed during Fe deficiency (6, 27, 30), we hypothesized that the bleaching observed in

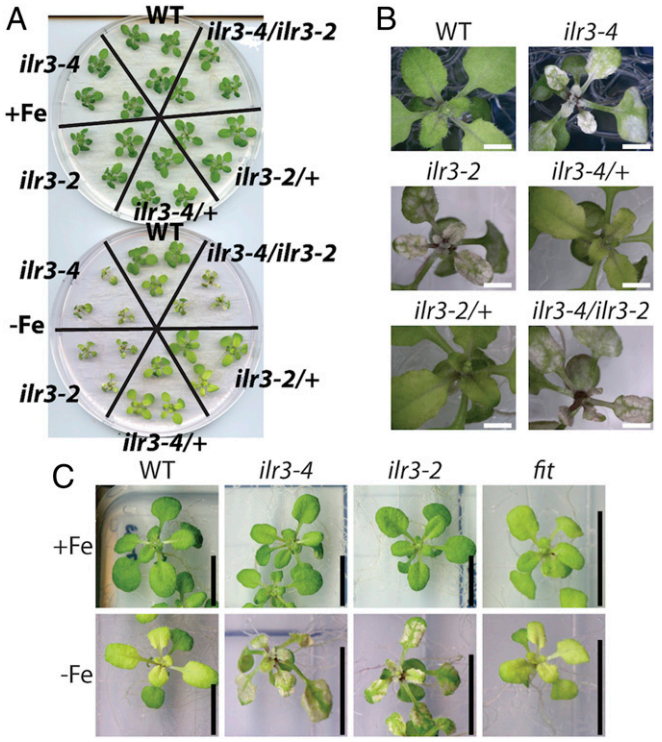

Fig. 3. The leaves of *ilr3-4* mutants bleach during Fe deficiency. (*A*) Two-week-old WT, *ilr3-4*, *ilr3-2*, *ilr3-4*/+, *ilr3-2*/+, and *ilr3-4*/*ilr3-2* mutant plants were transferred to Fe-deficient or Fe-sufficient media for 6 d. (*B*) Loss of *ILR3* results in leaf bleaching during Fe deficiency. Stereomicroscopy images of representative Fe-deficient plants shown in *A*. (Scale bars, 1 cm.) (*C*) Leaves of *ilr3-2* and *ilr3-4* plants develop leaf bleaching atypical of Fe-deficient plants. Two-week-old WT, *ilr3-2*, *ilr3-4*, and *fit-2* plants were transferred to Fe-sufficient or Fe-deficient media for 6 d. (Scale bars, 1 cm.)

ilr3-4 could be attributed to phototoxicity. We therefore tested whether light was required for bleaching in *ilr3-4* by growing plants under low-light conditions, achieved by shading the plants with mesh screening (~30 µmol photons m^{-2} s^{-1} under shade vs. ~120 µmol photons m^{-2} s^{-1} under normal lighting). After 6 d on Fe-deficient medium, leaves from low-light–grown *ilr3-4* mutant plants did not show the bleaching symptoms seen in *ilr3-4* mutants grown under normal light conditions (Fig. 4*A*). We also compared plants grown under short-day conditions (8 h light/16 h dark) to plants grown under long-day conditions (16 h light/8 h dark, the typical condition used in this study). Similar to the shading experiment, leaves of *ilr3-4* mutants did not bleach after 6 d of growth on Fe-deficient medium under short-day conditions (Fig. 4*B*). These experiments indicate that light is necessary for bleaching and that *ILR3* is necessary for photoprotection during Fe deficiency.

Due to the mottled bleaching in *ilr3-4* leaves during Fe deficiency, we questioned whether there would also be a corresponding change in the distribution of metals in Fe-deficient *ilr3-4* leaves. To address this question, we performed synchrotron X-ray fluorescence (SXRF) on leaves of *ilr3-4* plants transferred to Fe-deficient medium for 4 d. We observed a striking redistribution of the macronutrients potassium (K) and calcium (Ca) in *ilr3-4* leaves (Fig. 5 *A* and *B*), with Ca being enriched in the bleached leaf portions compared to the surrounding green portions, while K exhibited the opposite distribution, being strongly depleted in the bleached portions. However, there was no noticeable difference in the Fe levels between the bleached and healthy tissue in *ilr3-4* leaves (Fig. 5 *A* and *B*). Unlike in *ilr3-4* leaves, there is no redistribution of Ca and K in WT leaves (Fig. 5 *A* and *B*).

Subgroup IVc Transcription Factors Have Diverged Functions in Shoots. *ILR3* is a member of the subgroup IVc bHLH transcription factor family. In addition to *ILR3*, the other three members of this subfamily, *bHLH115*, *bHLH104*, and *bHLH34*, have all been shown to be positive regulators of the subgroup Ib bHLH transcription factors during Fe deficiency in roots and function additively to confer resistance to Fe deficiency (14–16). To gain further insight into the relationships among these transcription factors, we generated a phylogenetic tree to infer their evolutionary history using representatives of major eudicot and grass lineages as well as the moss *Physcomitrella patens* (*SI Appendix*, Fig. S2). Surprisingly, while all four of these transcription factors regulate the expression of the subgroup Ib bHLH transcription factors during Fe deficiency, the subgroup IVc bHLH transcription factors diverged early in the angiosperm lineage. The duplication leading to the divergence of the *ILR3*/*bHLH115* subclade and the *bHLH104*/*bHLH34* subclade likely occurred before the divergence of the eudicot and grass lineages, with *Aquilegia coerulea*, the most basal eudicot species in our analysis, retaining a copy from each subgroup IVc subclade. *bHLH104* and *bHLH34* diverged more recently in the *Brassicacae* lineage. While the *ILR3*/*bHLH115* subclade may have also duplicated in the *Brassicacae*, strong conclusions are difficult to reach because of poor bootstrap support. Regardless, because the duplications that gave rise to the different subgroup IVc transcription factors occurred relatively early in angiosperm history, it is possible that they have diverged in function. We thus tested whether *bhlh115-2*, *bhlh34*, or *bhlh104-2* mutants were photosensitive during Fe deficiency like *ilr3-4* or whether *ILR3* had adopted a unique function. While *bhlh115-2*, *bhlh34*, or *bhlh104-2* mutants developed chlorosis after transfer to Fe-deficient conditions, none of them developed leaf bleaching like *ilr3-4* or *ilr3-2* mutants (Fig. 6 *A* and *B*), indicating that *ILR3* plays a unique, nonredundant role in leaves among the subgroup IVc bHLH transcription factors. The sensitivity of the bHLH IVc mutants to Fe deficiency was also tested by germinating seeds directly on minimal medium that lacks Fe or minimal medium supplemented with either Fe (+Fe) or ferrozine (−Fe). All genotypes tested exhibited normal growth on medium containing 50 µM Fe (*SI Appendix*, Fig. S3). On minimal medium without Fe, we observed strong growth inhibition of *ilr3-2* and *ilr3-4* mutants, but minimal effect on WT, *bhlh104-2*, *bhlh115-2*, and *bhlh34* mutants (*SI Appendix*, Fig. S3). In the presence of 50 µM ferrozine, all genotypes showed chlorosis and mutants for all four bHLH IVc transcription factors exhibited worse growth than WT (*SI Appendix*, Fig. S3).

Given that *ilr3-4* displays a unique leaf bleaching phenotype and shows strong growth inhibition on minimal medium compared to

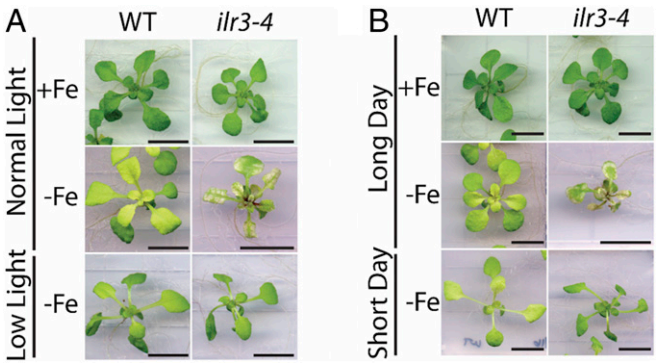

Fig. 4. Bleaching in *ilr3-4* mutants is light dependent. (*A*) Low-light intensity suppresses leaf bleaching in *ilr3-4* plants. Two-week-old plants were transferred to Fe-sufficient, Fe-deficient, or Fe-deficient medium with shade under mesh screening for 6 d. (Scale bars, 1 cm.) (*B*) Short daylength suppresses bleaching in *ilr3-4*. Two-week-old plants were transferred to Fe-sufficient or Fe-deficient medium and grown under either 16 h light/8 h dark or 8 h light/16 h dark for 6 d. (Scale bars, 1 cm.)

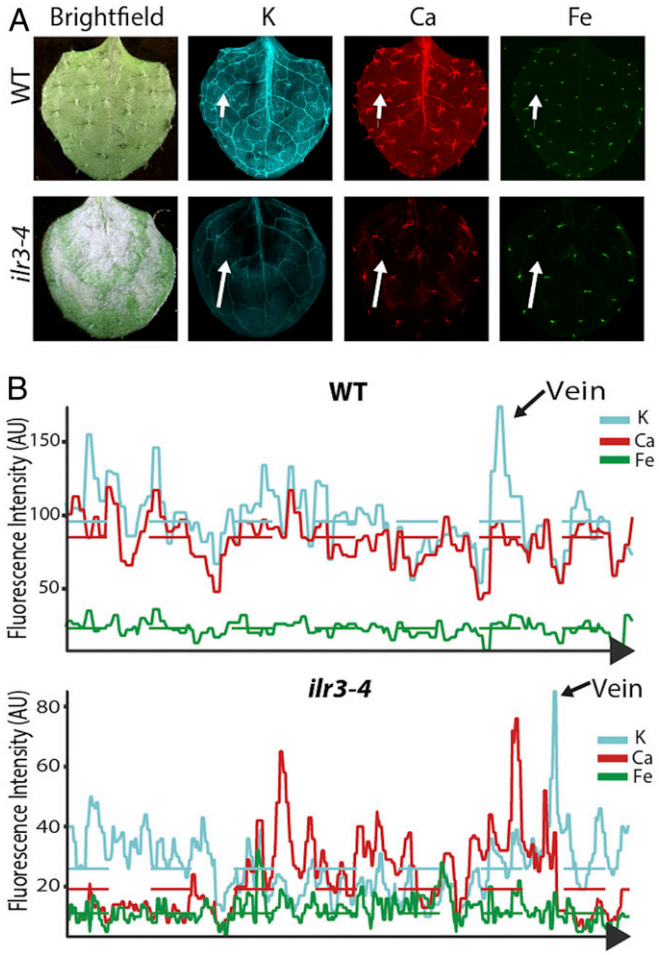

Fig. 5. Bleaching in *ilr3-4* leaves is accompanied by redistribution of subset of ions. (*A*) SXRF scans showing K, Ca, and Fe localization and distribution in the first true leaf of bleached *ilr3-4* and in a wild-type leaf. Two-week-old plants were transferred to Fe-deficient medium for 4 d prior to imaging. A brightfield photo of the imaged leaf is shown. (*B*) The intensity profile plots arbitrary fluorescence intensity of K, Ca, and Fe through the arrow shown in the SXRF images. The horizontal dashed line indicates the median fluorescence intensity and the fluorescence peak corresponding to a vein is labeled. Note that the intensities for K, Ca, and Fe are scaled independently.

bhlh115-2, *bhlh34*, and *bhlh104-2*, we hypothesized that gene expression changes would also differ between these mutants and *ilr3-4* under Fe deficiency. To test this hypothesis, we measured gene expression in leaves of plants grown with or without Fe using a Nanostring probeset comprising probes for 11 Fe-regulated genes that are expressed in shoots as well as *ILR3*, *bHLH115*, and *bHLH104*.

Expression of the subgroup Ib bHLH transcription factors was below the detection threshold in Fe-sufficient plants for all genotypes tested (Fig. 6*C*). During Fe deficiency, expression of all subgroup Ib bHLH transcription factors was lower in *ilr3-4* mutants compared to WT (Fig. 6*C*). Similarly, the expression of all subgroup Ib transcription factors was lower in *bhlh104-2* mutants compared to WT. However, misregulation of the subgroup Ib BHLH transcription factors was significantly weaker in *bhlh115-2* mutants; only *bHLH39* and *bHLH101* expression was reduced in *bhlh115-2* compared to WT plants. We did not detect any misregulation of the subgroup Ib bHLH transcription factors in *bhlh34* shoots.

We observed similar trends in the regulation of other Fe deficiency–induced genes. Expression of *BTS* was lower in *ilr3-4* and *bhlh104-2* mutant leaves during Fe deficiency, while *BTS* expression was unchanged in *bhlh115-2* and *bhlh34* mutants (Fig. 6*C*). *OLIGOPEPTIDE TRANSPORTER3* (*OPT3*) expression was only slightly reduced in *bhlh104* mutants compared to WT while there were no differences in *OPT3* expression between WT and *ilr3-4*, *bhlh115-2*, and *bhlh34* (*SI Appendix*, Fig. S4). *FERREDOXIN1* (*Fd1*) induction was impaired only in *ilr3-4* during Fe deficiency (*SI Appendix*, Fig. S4). Collectively, our NanoString results indicate that *ILR3* and *bHLH104* are the most critical subgroup IVc transcription factors, with *bHLH115* playing a more minor role and *bHLH34* not appearing to be involved in the shoot Fe deficiency response.

Our NanoString probeset contains probes for the detection of two Fe deficiency–repressed genes, *FER1* and *STROMAL ASCORBATE PEROXIDASE* (*SAPX*). The expression levels of these genes were similar in *bhlh115-2*, *bhlh104-2*, and *bhlh34*, compared to WT regardless of Fe treatment (Fig. 7*C*). However, *FER1* expression was higher in *ilr3-4* mutants compared to WT under all conditions, whereas *SAPX* expression was similar to WT during Fe sufficiency but was not repressed during Fe deficiency in *ilr3-4* mutants. Expression of Fe deficiency–repressed genes thus highlights that among the subgroup IVc bHLHs, *ILR3* is unique in its role as a repressor during Fe deficiency.

***POPEYE* Is Required for Phototolerance.** *ILR3* is required for phototolerance as well as repression of Fe-regulated genes, whereas its paralogs are not required for either. While the subgroup IVc transcription factors have been proposed to form functional heterodimers, an additional bHLH transcription factor, *POPEYE* (*PYE*), has also been shown to interact with *ILR3* and its paralogs (20). *PYE* has previously been shown to attenuate the expression of Fe deficiency–induced genes, indicating that it is a transcriptional repressor (20). We thus hypothesized that *PYE* may also be required for the repression of Fe deficiency–repressed genes in shoots.

We compared gene expression changes between WT and *pye* mutants (Fig. 7*A* and *SI Appendix*, Fig. S5). All Fe deficiency–inducible genes were properly induced in *pye* except for *PYE*, which was below the detection threshold in the *pye* mutant background, and *FD1*, whose expression was not induced during Fe deficiency similar to *ilr3-4* mutants (*SI Appendix*, Fig. S5). However, similar to *ilr3-4* mutants, repression of *SAPX* and *FER1* during Fe deficiency was *PYE* dependent. Ferritin protein levels were also derepressed in *ilr3-2*, *ilr3-4*, and *pye* mutants compared to WT (*SI Appendix*, Fig. S6), although ferritin expression was still lower in Fe deficiency compared to Fe sufficiency. The results indicate that PYE does act as a repressor of Fe deficiency–repressible genes.

Because *pye* mutants exhibit misregulation of Fe deficiency–repressed genes in shoots, we asked whether *pye* mutants exhibited a physiological shoot phenotype during Fe deficiency similar to *ilr3-4*. After being transferred to Fe-deficient conditions for 6 d, leaf bleaching was apparent on *pye* mutant leaves, although the extent of bleaching was less severe than in *ilr3-4* mutants (Fig. 7*B*). Furthermore, the leaf bleaching in *pye* mutants could be suppressed under low light (Fig. 7*B*), indicating that bleaching in *pye* mutants is due to photosensitivity.

Given that *ilr3-4* and *pye* mutants exhibit photosensitivity, we tested whether photosynthetic efficiency was compromised in these mutants using chlorophyll fluorometry. During Fe deficiency, both F_v/F_m (the maximum PSII efficiency) and F_q'/F_m' (the steady-state PSII efficiency) were reduced in WT (Fig. 7*C*), although the reduction of F_q'/F_m' was greater than the reduction in F_v/F_m, as has been reported previously in other species (5, 29). F_v/F_m was reduced even further in the *ilr3-4* and *pye* mutants compared to WT, indicating a greater loss of PSII efficiency and suggesting photodamage at PSII's reaction center. F_q'/F_m' was also reduced to a greater extent in *ilr3-4* mutant plants compared to WT plants (Fig. 7*C*). Interestingly, while the reduction in F_v/F_m in *pye* mutant plants was greater than in WT, F_q'/F_m' was higher in *pye* compared to WT during Fe deficiency (Fig. 7*C*), indicating that *pye* maintains higher steady-state PSII efficiency

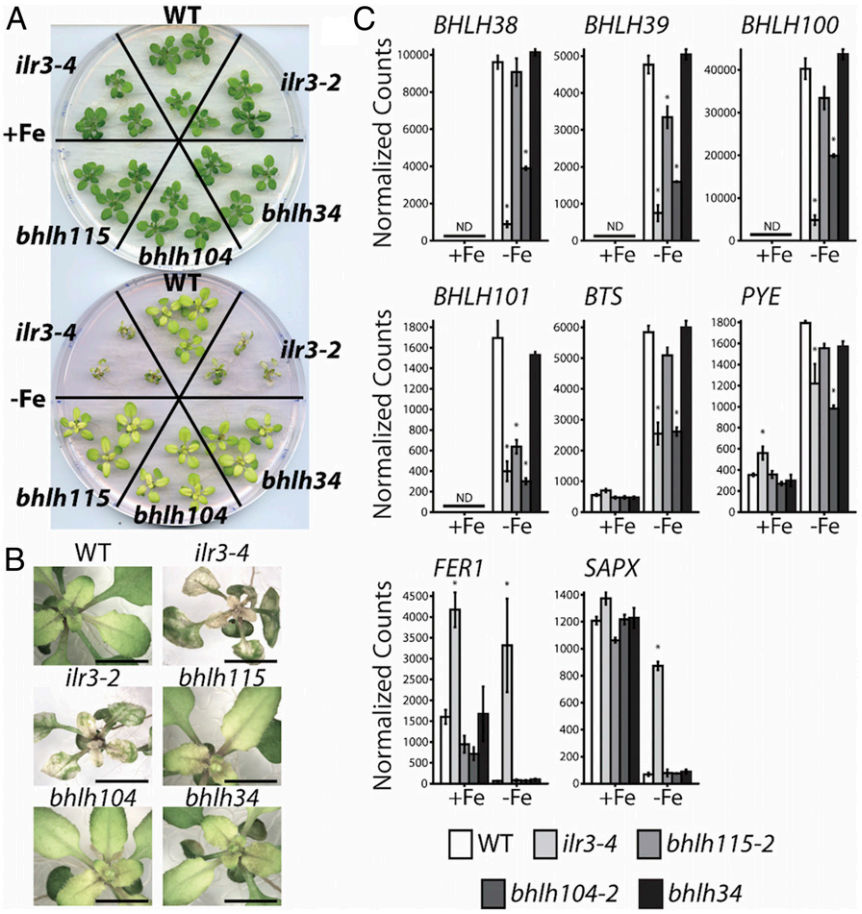

Fig. 6. Paralogs of *ILR3* are not required for phototolerance during Fe deficiency and have varying roles in controlling iron-regulated gene expression in the shoots. (*A*) Growth comparison of WT, *ilr3-4*, *bhlh115-2*, *bhlh104-2*, and *bhlh34* under Fe-deficient and Fe-sufficient conditions. Plants grown on 1/2 strength B5 medium for 2 wk were transferred to Fe-deficient or Fe-sufficient conditions for 6 d. (Scale bars, 1 cm.) (*B*) Close-up photographs of plants from *A*. (Scale bars, 1 cm.) (*C*) Gene expression analysis of shoots of subgroup IVc bHLH transcription factor mutants. Plants grown on 1/2 strength B5 for 2 wk were transferred to Fe-sufficient or Fe-deficient conditions for 3 d. RNA was extracted from leaves and gene expression was measured using NanoString ($n = 3$). Asterisks indicate significant differences ($P < 0.05$) from WT plants grown under the same condition by Dunnet's test. ND, not detected.

despite the loss of efficiency at the PSII reaction center. Regardless, our results are indicative of damage and photoinhibition at the PSII reaction center in *ilr3-4* and *pye* mutants.

Singlet Oxygen Accumulates in *ilr3-4* and *pye* Mutants during Fe Deficiency. Light-dependent cell death is mediated by ROS. Phototoxicity can lead to the accumulation of multiple forms of ROS, including singlet oxygen and hydrogen peroxide (37). Both of these forms of ROS can induce programmed cell death (PCD), although they do so by independent mechanisms and can be distinguished by changes in gene expression of different ROS-responsive marker genes (38, 39). To determine which form of ROS was responsible for bleaching, we measured the expression of various ROS-induced genes in WT, *ilr3-4*, and *pye* plants. During Fe deficiency, expression of *OXI1*, a generic oxidative stress marker that is induced by both singlet oxygen and hydrogen peroxide, was not induced in WT but was strongly induced in *ilr3-4* and *pye* (Fig. 8*A*), consistent with the strong stress phenotype observed in these mutants. We also measured the expression of two genes specifically induced by singlet oxygen (*BAP1* and *At3g01830*) as well as two genes specifically induced by hydrogen peroxide (*MAPK6* and *PTI1-4*) (38, 39). Both *BAP1* and *At3g01830* were strongly induced in *ilr3-4* and *pye* mutants but not WT during Fe deficiency (Fig. 8*A* and *SI Appendix*, Fig. S7). However, neither *MAPK6* nor *PTI1-4* were induced in either *ilr3-4* or *pye* (Fig. 8*A* and *SI Appendix*, Fig. S7). The specific induction of *BAP1* and *At3g01830* suggests that *ilr3-4* and *pye* accumulate singlet oxygen during Fe deficiency. We also measured the expression of *At3g01830* in the *bhlh115-2*, *bhlh104-2*, and *bhlh34* mutants. Consistent with their lack of bleaching, *At3g01830* expression was not induced in these mutants during Fe deficiency (*SI Appendix*, Fig. S8).

To further support the gene expression results in *ilr3-4* mutants, the fluorescent stain Singlet Oxygen Sensor Green (SOSG) was used to detect the production of singlet oxygen in *ilr3-4* and *pye* mutants. After exposure to high light (~500 μmol m^{-2} s^{-1} for 30 min), fluorescent signal from SOSG could not be detected in WT, *ilr3-4*, or *pye* mutants grown on Fe-sufficient medium (Fig. 8*B*). During Fe deficiency, staining was not observed in WT (Fig. 8*B*). However, strong staining was observed in both *ilr3-4* and *pye* mutants, indicating that these two mutants accumulate singlet oxygen during Fe deficiency.

Singlet oxygen preferentially reacts with molecules that contain double bonds, such as polyunsaturated fatty acids, carotenoids, and the amino acids histidine (His) and tryptophan (37). Exogenous His has also been shown to protect plants against singlet oxygen stress (39, 40). Supplementing Fe-deficient medium with 2 mM His was able to suppress leaf bleaching in both *ilr3-4* and *pye* mutants (Fig. 8*C*), further verifying the accumulation of singlet oxygen in these mutants. The mutant plants still bleached, however, on Fe-deficient medium containing 2 mM arginine (Fig. 8*C*),

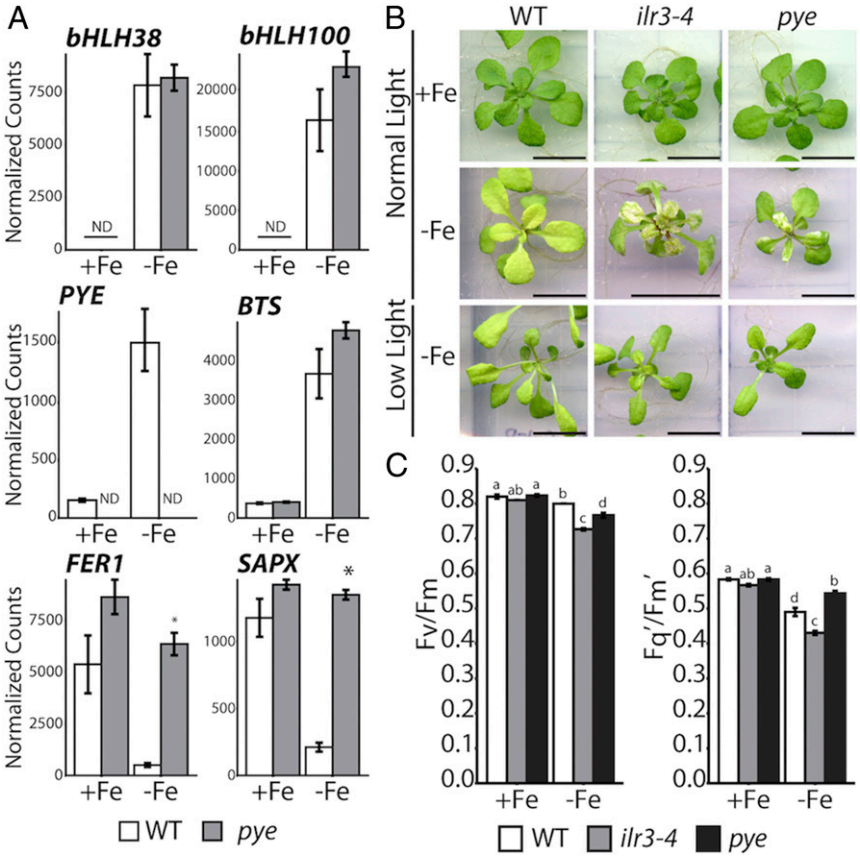

Fig. 7. *PYE* is required for regulation of repressed genes in shoots and phototolerance during Fe deficiency. (*A*) Gene expression analysis of *pye* mutant shoots. Plants grown on 1/2 strength B5 for 2 wk were transferred to Fe-sufficient or Fe-deficient conditions for 3 d. RNA was extracted from leaves and gene expression was measured using NanoString ($n = 3$). Asterisks indicate significant differences ($P < 0.05$) from WT plants grown under the same condition by Student's *t* test. ND, not detected. (*B*) *pye* mutants bleach during Fe deficiency and are rescued by low light. WT, *ilr3-4*, and *pye* plants grown on 1/2 strength B5 medium for 2 wk were transferred to Fe-sufficient conditions, Fe-deficient conditions, or Fe-deficient conditions under shade for 6 d. (Scale bars, 1 cm.) (*C*) *ilr3-4* and *pye* mutants have reduced maximum photosynthetic efficiency during Fe deficiency. WT, *ilr3-4*, and *pye* mutants grown on 1/2 strength B5 medium for 2 wk were transferred to Fe-sufficient or Fe-deficient conditions for 3 d. The maximum PSII efficiency (F_v/F_m) and steady-state PSII efficiency (F_q'/F_m') were measured from whole rosettes. Different letters indicate $P < 0.05$ by Tukey's test.

excluding the possibility that the additional nitrogen provided by the His was responsible for the rescue.

***ILR3* and *PYE* Are Required for Drana Destacking during Fe Deficiency.** Because *ilr3* and *pye* mutants are photosensitive during Fe deficiency, we examined whether chloroplast ultrastructure was altered in these mutants during Fe deficiency. We selected leaves 3 and 4 from plants grown for 6 d on Fe-sufficient or Fe-deficient media, which were either chlorotic in the case of WT or bleached in the case of *ilr3-4* and *pye* mutants. Unbleached portions of the leaves were used to image chloroplasts. In WT, we observed strong perturbations in chloroplast ultrastructure (Fig. 9*A*). Fewer grana were observed in Fe-deficient plants, and tall grana stacks were absent during Fe deficiency, resulting in a 50% reduction in median grana height (Fig. 9*B*). Surprisingly, the chloroplasts from *ilr3-4* and *pye* mutants did not seem altered in anyway. The chloroplasts of both mutants contained abundant grana with no loss of large grana (Fig. 9 *A* and *B*). We also quantified the number of plastoglobules as a potential factor in membrane remodeling. We did not detect differences across genotypes or between Fe-sufficient and Fe-deficient plants (*SI Appendix*, Fig. S9).

We next examined whether the integrity of photosynthetic complexes had also remained intact by blue native polyacrylamide gel electrophoresis (BN-PAGE) analysis of thylakoid protein complexes. As reported for spinach (41), no obvious qualitative differences were observed between Fe-sufficient and Fe-deficient WT (*SI Appendix* Fig. S10). In *ilr3-4* mutants, however, there was a notable loss of the LHCII assembly and LHCII trimer complexes that are enriched in grana. In *pye* mutants, however, there was no significant loss of any complex, correlating with the weaker photosensitivity of *pye* mutants compared to *ilr3-4* mutants.

***ILR3* and *PYE* Enhance PSII Turnover and Repair during Fe Deficiency.** Grana destacking is a regulated process that responds to changes in light intensity to facilitate PSII repair (42–45). When PSII is photodamaged, the PSII subunit D1 becomes oxidized and the PSII repair machinery removes and degrades the damaged D1 protein and PSII is reassembled with properly functioning de novo translated D1 protein (46). Grana destacking increases the rate of PSII repair by increasing the exposure of PSII, which is enriched in grana, to the repair machinery, which is excluded from grana (47). We thus hypothesized that the smaller grana in Fe-deficient WT plants enhances the rate at which PSII is repaired.

The rate of PSII repair was assessed by inhibiting chloroplast translation with the chloroplast ribosomal inhibitor lincomycin and monitoring the levels of D1 protein over 8 h in the light. Over the time course, we did not detect a noticeable decrease in D1 protein levels in Fe-sufficient WT, and there was no difference in D1 levels between Fe-sufficient and Fe-deficient WT plants at T0 (Fig. 9*C*). However, D1 protein levels were reduced in Fe-deficient WT plants after 8 h in the light in the presence of

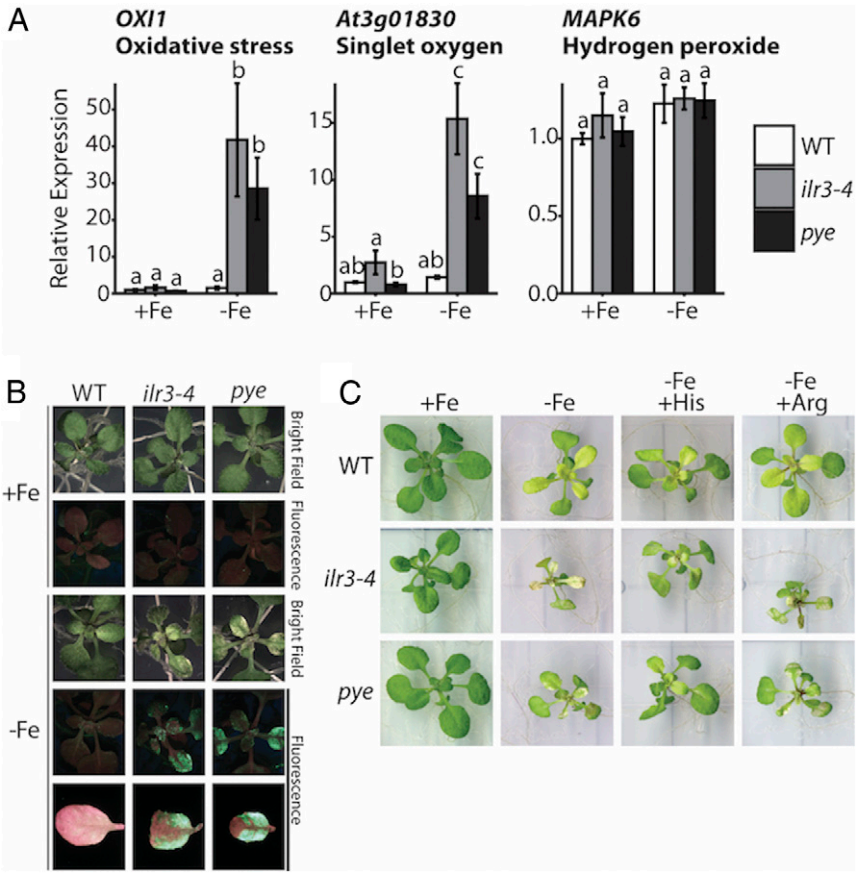

Fig. 8. *ilr3-4* and *pye* mutants accumulate singlet oxygen during Fe deficiency. (*A*) Gene expression analysis of ROS-induced marker genes. Plants grown for 2 wk on 1/2 strength B5 medium were transferred to Fe-sufficient or Fe-deficient conditions for 5 d. RNA was extracted from shoots for qPCR analysis ($n = 3$). (*B*) Singlet oxygen detection by SOSG. Two-week-old plants grown on 1/2 strength B5 medium were transferred to Fe-sufficient or Fe-deficient conditions for 3 d and stained with SOSG and illuminated for 30 min at 500 μmol photons m^{-2} s^{-1}. SOSG fluorescence is shown in green while chlorophyll fluorescence is shown as red. (*C*) Bleaching in *ilr3-4* and *pye* can be rescued with histidine. Two-week-old plants were transferred to Fe-sufficient medium, Fe-deficient medium, or Fe-deficient medium supplemented with either 2 mM histidine or 2 mM arginine. Plants were then grown for 6 additional days.

lincomycin, indicating that D1 turnover is higher in Fe-deficient than in Fe-sufficient plants. The amount of the large subunit of Rubisco (RbcL), however, did not change in response to lincomycin treatment, indicating that increased turnover of D1 during Fe deficiency is specific. In *ilr3-4* and *pye* mutants, the levels of RbcL were similar to WT plants under both Fe-sufficient and Fe-deficient conditions (Fig. 9*B*). However, D1 protein levels did not diminish in the presence of lincomycin in Fe-deficient *ilr3-4* and *pye*, indicating that the D1 protein is not turning over and thus PSII repair is not accelerated in *ilr3-4* and *pye* during Fe deficiency.

Discussion

The Fe deficiency response is regulated by many bHLH transcription factors (9, 10, 13–19, 26). In this study, we demonstrate that *ilr3-4* is able to suppress the *bts* mutant phenotypes (Figs. 1 and 2), providing direct evidence that ILR3 acts downstream of BTS to induce the expression of the subgroup Ib bHLH transcription factors in roots. While it shares this function with its paralogs (14–16), ILR3 plays a more significant role in shoots than its paralogs (Fig. 10). Not only is the induction of the subgroup Ib transcription factors in shoots more severely compromised in *ilr3-4* compared to *bhlh115-2*, *bhlh104-2*, and *bhlh34* mutants, but *ILR3* is also required for the repression of Fe deficiency–repressed genes, while *bHLH115*, *bHLH104*, and *bHLH34* are dispensable for transcriptional repression of *FER1* and *SAPX* (Fig. 6*C*). Additionally, the subgroup IVb bHLH transcription factor *PYE* is also required for the repression of these genes in shoots during Fe deficiency (Fig. 7*A*), in addition to its previously described role as an attenuator of gene induction in roots (20). Given that PYE and ILR3 have been shown to physically interact (20, 22), our results suggest that PYE and ILR3 may heterodimerize to form a repressor complex, while ILR3 may heterodimerize with bHLH115, bHLH104, or bHLH34 to form an activator complex, in addition to being able to form an activating complex with URI (18, 19). Our results are consistent with recent work demonstrating that ILR3 and PYE, but not bHLH115, bHLH104, or bHLH34, are required for the repression of *FERRITIN* genes during Fe deficiency (21).

Chloroplasts are the major sink for foliar Fe (1), and many studies have demonstrated the adverse effects of Fe deficiency on photosynthesis (4–6, 27–29, 31, 41, 48). All studies have demonstrated that Fe deficiency has a weak impact on PSII's maximum efficiency (F_v/F_m) but a large impact on PSII's steady-state efficiency (F_q'/F_m'), indicating that while the PSII reaction center is relatively unharmed, electron flow through PSII to cytochrome b_6f is strongly disrupted. While PSI activity has been known to be more strongly reduced than PSII activity during Fe deficiency (49, 50), the acceptor side efficiency of PSI, which contains multiple Fe cofactors (51), is not affected by Fe deficiency (6, 52). Furthermore, the primary acceptor quinone Q_A at PSII has been shown to be overreduced during Fe deficiency (27, 52), which may be due to loss of the Fe atom located between the two quinones in PSII (53). These studies collectively suggest that

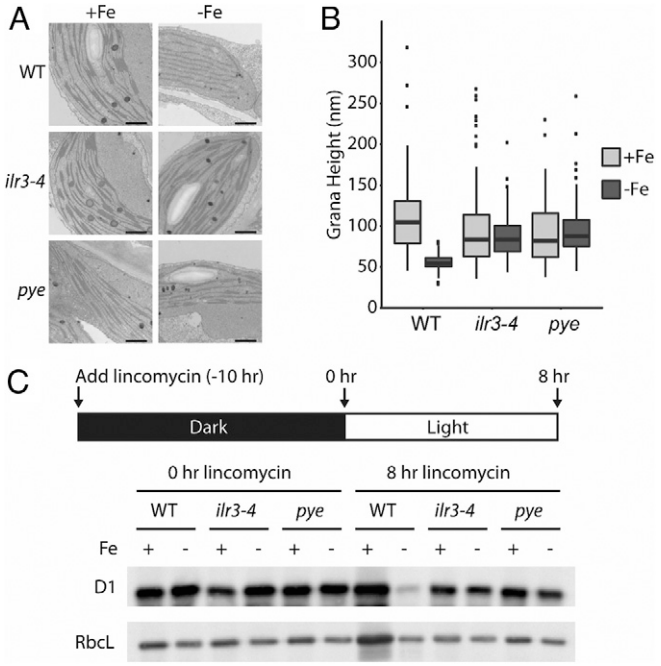

Fig. 9. *ILR3* and *PYE* are necessary for thylakoid restructuring and PSII repair during Fe deficiency. (*A*) Transmission electron microscopy (TEM) of chloroplasts from leaves 3 and 4 of WT, *ilr3-4*, and *pye* plants after 6 d on Fe-deficient or Fe-sufficient medium. (Scale bar, 200 nm.) (*B*) Quantification of grana height from TEM images ($n \geq 45$ grana from five to six chloroplasts). The line in the box denotes the median value, while the box contains the 25th to 75th percentiles. Whiskers mark the highest and lowest values excluding outliers (marked as black dots). Outliers are defined as greater or less than the 75th or 25th percentile, respectively, by 1.5 times the interquartile range. (*C*) D1 turnover increases during Fe deficiency and is dependent on ILR3 and PYE. Two-week-old plants grown on 1/2 strength B5 medium were transferred to Fe-deficient or Fe-sufficient medium for 5 d and incubated in 1 mM lincomycin overnight in the dark. Shoots were harvested in the morning (0 h) or 8 h after transfer to light (8 h). Western blotting was performed against D1 and RbcL, with RbcL serving as a loading control.

the primary electron transfer bottleneck occurs upstream of PSI, resulting in overreduction of PSII, which favors the production of singlet oxygen (54).

The sensitization of plants to singlet oxygen production during Fe deficiency has not previously been shown. Photosensitivity during Fe deficiency, however, has been demonstrated in both land plants and algae. Photosensitivity in land plants has been demonstrated in the light-sensitized barley mutant *chlorina*, which cannot synthesize chlorophyll *b* and thus lacks LHCII and the ability to dissipate excess light energy by nonphotochemical quenching (55). During Fe deficiency, *chlorina* mutants exhibit photobleaching at light intensities tolerated by Fe-sufficient *chlorina* mutant plants (31), indicating that the plants are sensitive to photooxidative stress during Fe deficiency. In the diatom *Phaeodactylum tricornutum*, strong photoinhibition occurs during Fe deficiency at elevated light intensities that do not affect Fe-replete cells (52). Recent work has demonstrated that Zn-deficient plants are also photosensitive and that autophagy is required to mobilize Zn to prevent the production of light-dependent ROS (56), highlighting that low metal availability raises the propensity of the photosynthetic machinery to generate ROS. It is clear that disruption of the photosynthetic machinery results in photosensitivity; the mechanism by which plants can mitigate light stress during Fe deficiency, however, is unknown.

Here, we demonstrate that *ILR3* and *PYE* are required to confer photoprotection during Fe deficiency. Extensive photobleaching was observed in *ilr3-2*, *ilr3-4*, and *pye* mutants (Figs. 3 and 6*B*), and photobleaching could be suppressed by reducing either the light intensity or daylength (Figs. 4 and 7*B*). We also determined that photobleaching in *ilr3-4* and *pye* mutants was due to the accumulation of the ROS singlet oxygen rather than hydrogen peroxide (Fig. 8), indicating that the primary site of photoinduced ROS in Fe-deficient *ilr3-4* and *pye* mutants is photosystem II (PSII), given that PSI cannot generate singlet oxygen (54). Generation of singlet oxygen is consistent with the loss of PSII steady-state efficiency (5, 6, 41) and the observation that electron transfer from Q_A^- to Q_B is strongly inhibited during Fe deficiency in lettuce (27), which results in the electron back reactions that lead to the production of singlet oxygen (54, 57).

We observed a redistribution of ions that occurred during the bleaching of *ilr3-4* plants during Fe deficiency, with a strong depletion in K but enrichment of Ca in bleached sectors compared to surrounding healthy tissue (Fig. 5). Because of the loss of cellular integrity and cell death that was observed in the bleached leaf portions, ion leakage may contribute to the loss of K from the bleached sectors. The cause of the high Ca concentration, however, is less clear. Ca is a known regulator of programmed cell death in plants (58). Thus, one possible explanation for the Ca distribution is that excess Ca is deposited into cells that accumulate high amounts of singlet oxygen, and this large influx of Ca triggers programmed cell death. The mechanism that results in the retention of Ca in the bleached tissue but not K, however, is still unclear.

The transcription factors *FIT*, *bHLH115*, *bHLH104*, and *bHLH34*, are not required for phototolerance (Fig. 6*A*). We can thus conclude that 1) deregulation of root Fe uptake is insufficient to cause phototoxicity, and 2) *ILR3* has diverged significantly from its paralogs to adopt a novel and unique function. We note that ILR3 and PYE have been reported to function in a regulatory network that controls the response to wounding pathogens by modulating glucosinolate accumulation under Fe deficiency (59, 60). *bHLH115*, *bHLH104*, and *bHLH34* may also have independent functions, although we have been unable to find a distinctive phenotype for *bhlh115*, *bhlh104*, or *bhlh34* single mutants. Given that photobleaching in *ilr3-4* and *pye* was only apparent under long-day conditions under moderate light and the severe growth inhibition of *ilr3-4* when germinated on Fe-deficient medium provides no information in terms of phototoxicity

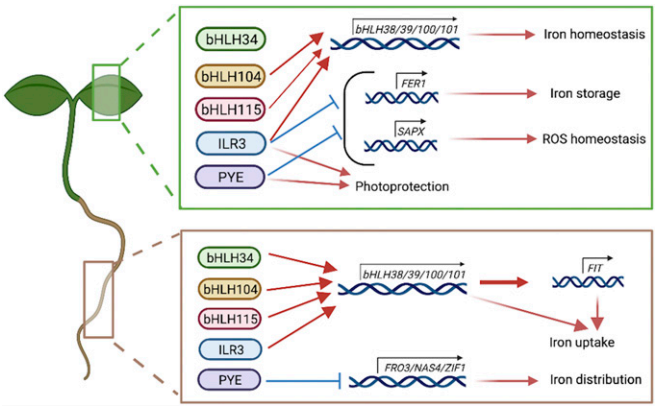

Fig. 10. Model of subgroup IVc bHLH and PYE function during Fe deficiency. In roots, the subgroup IV bHLH transcription factors regulate iron uptake, while PYE represses the expression of genes involved in Fe utilization and distribution. In shoots, ILR3 and bHLH104 play a more prominent role in regulating the expression of bHLH Ib transcription factors compared to bHLH115, while ILR3 and PYE promote photoprotection and repress the expression of Fe deficiency–repressible genes that mediate iron storage and ROS homeostasis. This figure was created with http://BioRender.com.

(*SI Appendix*, Fig. S3), it is likely that that any divergent function of *bHLH115*, *bHLH104*, or *bHLH34* would only be observable under the correct experimental conditions.

While grana height is significantly reduced in WT plants during Fe deficiency, grana height is not altered in *ilr3-4* and *pye* mutants (Fig. 9). At the ultrastructural level, chloroplasts from *ilr3-4* and *pye* mutants appeared remarkably healthy, even those from leaves that were bleaching. This observation suggests that Fe deficiency–dependent perturbation of chloroplast ultrastructure is at least in part genetically controlled by ILR3 and PYE rather than a consequence of the loss of Fe cofactors. Our results are consistent with the proposal that the loss of the activity of some Fe-dependent processes is due to retuning the cellular Fe economy rather than Fe depletion per se (6, 7, 61). In this scenario, reduction in grana stacking could spare Fe from the photosynthetic machinery to be prioritized for use in other proteins. ILR3/PYE-dependent repression of genes encoding Fe-containing proteins such as *SAPX* and *FER1* are also likely a component of an Fe sparing strategy.

Grana have been proposed to serve multiple functions, notably the enrichment of PSII and LHCII, which facilitates the formation of PSII/LHCII megacomplexes that maximize light absorption (44, 62). At the same time, grana formation also results in the segregation of PSII/LHCII from other thylakoid protein complexes, including PSI/LHCI and the PSII repair machinery (47, 63). Alterations in grana stacking are thus an important aspect of minimizing photooxidative stress. Phosphorylation of LHCII and PSII by the light-dependent kinases STN7 and STN8, for example, reduces grana stacking, and both the phosphorylation events and the reduction in grana stacking are necessary to increase the rate of PSII repair (64). However, neither *STN7* nor *STN8* are transcriptionally regulated by Fe (65), and whereas Fe-deficient plants have grana that are shorter in height (Fig. 9*B*), STN7/STN8 control grana diameter rather than height (64). Fe deficiency–induced changes in thylakoid ultrastructure thus seem to be independent of known PSII/LHCII phosphorylation-dependent mechanisms. Grana destacking can also protect again photooxidation by enhancing the efficiency of cyclic electron transfer (CET) around PSI (66), which acidifies the thylakoid lumen, resulting in increased nonphotochemical quenching (67, 68). Although the rate of CET increases in Fe-deficient plants (28), the total number of PSI reaction centers around which CET occurs decreases dramatically during Fe deficiency (4, 28, 30). The relative contributions of cyclic vs. linear electron transfer, and thus the potential role of grana stacking in enhancing CET and in promoting nonphotochemical quenching is unclear and requires more thorough analysis.

The degree of grana stacking has been demonstrated to correlate with light levels, with high light–adapted plants having grana with shorter height than low light–adapted plants (45). Plants grown under natural lighting (i.e., outdoor conditions where peak light intensity is very high) also have shorter grana than plants grown in controlled laboratory environments (45, 69), highlighting thylakoid plasticity under conditions that promote photooxidative stress. Partial unstacking has also been described in short-term high-light treatments in plants adapted to normal light intensities (42, 64). Furthermore, grana stacking has been shown to be a critical determinant of nitrogen deficiency tolerance in *Chlamydomonas reinhardtii*, as grana hyperstacking in the galactoglycerolipid lipase mutant *pgd1* causes severe chlorosis and poor growth during nitrogen deficiency and salinity stress due to a consequent imbalance in the PSII/PSI ratio (70). Galactoglycerolipids are the major lipids in thylakoid membranes, and grana hyperstacking in the *pgd1* mutant has been proposed to be due to the inability to degrade galactoglycerolipids into triacylglycerol (TAG). Interestingly, Fe-deficient *C. reinhardtii* cells accumulate more TAG than Fe-sufficient cells (71), suggesting that there may also be a link between grana destacking and Fe deficiency tolerance in *Chlamydomonas* as well. We hypothesize that grana destacking would have two consequences in Fe-deficient plants. First, loss of grana would thus lead to the dispersal of LHCII and PSII, reducing their proximity and the ability of energy to be efficiently transferred from LHCII to PSII. Second, the reduction in grana would increase the accessibility of damaged PSII to the PSII machinery that is excluded from grana (72), enhancing the rate of PSII repair. We observed greater D1 protein turnover in Fe-deficient WT plants compared to Fe-sufficient plants (Fig. 9*C*), indicative of increased PSII repair during Fe deficiency. However, D1 turnover was not responsive to Fe status in *ilr3-4* and *pye* (Fig. 9*C*), indicating that *ILR3* and *PYE* are necessary for up-regulating PSII repair during Fe deficiency. We thus propose that grana destacking mediated by *ILR3* and *PYE* during Fe deficiency increases the PSII repair rate, clearing chloroplasts of photodamaged PSII and thus mitigating the production of singlet oxygen.

Materials and Methods

Plant Materials and Growth Conditions. The *bts-3* (23), *ilr3-2* (73), *pye* (20), *bhlh115-2* (16), *bhlh104-1* (14), and *bhlh34* (15) were described previously. T-DNA mutants were obtained from the *Arabidopsis* Biological Resource Center. EMS mutagenesis, growth conditions, and media composition are described in *SI Appendix, SI Materials and Methods*.

Plant Phenotyping. The Fe chelate reductase assay, inductively coupled plasma mass spectrometry, photosynthetic efficiency, SOSG staining, synchrotron X-ray fluorescence, and electron microscopy are described in *SI Appendix, SI Materials and Methods*.

Protein Analysis. Details of protein extraction, thylakoid purification, lincomycin treatment, Western blotting, and blue native-PAGE are described in *SI Appendix, SI Materials and Methods*. Experiments were performed with either dissected shoots or dissected roots.

Gene Expression Analysis. RNA extraction, cDNA synthesis, and qRT-PCR are described in *SI Appendix, SI Materials and Methods*. NanoString PlexSet analysis was performed as described by the manufacturer. Normalization and detection limits are described in *SI Appendix, SI Materials and Methods*.

Data Availability. All study data are included in the article and/or supporting information.

ACKNOWLEDGMENTS. We thank Bob Schmitz for whole-genome resequencing and mapping, Louisa Howard and Chris Ogomo for electron microscopy, Eric Laderman for help with the D1 turnover experiments and Ryan Tappero for synchrotron imaging at X-ray Fluorescence Microprobe (XFM) beamline 4-BM of the National Synchrotron Light Source II, a US Department of Energy (DOE) Office of Science User Facility operated for the DOE Office of Science by Brookhaven National Laboratory under Contract DE-SC0012704. This work was supported by NSF grants IOS-1456290 and IOS-1257722 (to M.L.G.). G.Z.A. was the recipient of a Graduate Assistance in Areas of National Need fellowship from the US Department of Education.

1. N. Terry, G. Low, Leaf chlorophyll content and its relation to the intracellular localization of iron. *J. Plant Nutr.* **5**, 301–310 (1982).
2. A. Ben-Shem, F. Frolow, N. Nelson, Crystal structure of plant photosystem I. *Nature* **426**, 630–635 (2003).
3. Y. Umena, K. Kawakami, J.-R. Shen, N. Kamiya, Crystal structure of oxygen-evolving photosystem II at a resolution of 1.9 Å. *Nature* **473**, 55–60 (2011).
4. S. Spiller, N. Terry, Limiting factors in photosynthesis: II. Iron stress diminishes photochemical capacity by reducing the number of phototsynthetic units. *Plant Physiol.* **65**, 121–125 (1980).
5. A. Larbi, A. Abadía, F. Morales, J. Abadía, Fe resupply to Fe-deficient sugar beet plants leads to rapid changes in the violaxanthin cycle and other photosynthetic characteristics without significant de novo chlorophyll synthesis. *Photosynth. Res.* **79**, 59–69 (2004).
6. L. J. Hantzis *et al.*, A program for iron economy during deficiency targets specific Fe proteins. *Plant Physiol.* **176**, 596–610 (2018).
7. E. I. Urzica *et al.*, Systems and trans-system level analysis identifies conserved iron deficiency responses in the plant lineage. *Plant Cell* **24**, 3921–3948 (2012).
8. C. E. Blaby-Haas, S. S. Merchant, Regulating cellular trace metal economy in algae. *Curr. Opin. Plant Biol.* **39**, 88–96 (2017).

9. E. P. Colangelo, M. L. Guerinot, The essential basic helix-loop-helix protein FIT1 is required for the iron deficiency response. *Plant Cell* **16**, 3400–3412 (2004).
10. M. Jakoby, H.-Y. Wang, W. Reidt, B. Weisshaar, P. Bauer, FRU (BHLH029) is required for induction of iron mobilization genes in *Arabidopsis thaliana*. *FEBS Lett.* **577**, 528–534 (2004).
11. Y. X. Yuan, J. Zhang, D. W. Wang, H. Q. Ling, *AtbHLH29* of *Arabidopsis thaliana* is a functional ortholog of tomato *FER* involved in controlling iron acquisition in strategy I plants. *Cell Res.* **15**, 613–621 (2005).
12. Y. Yuan *et al*., FIT interacts with AtbHLH38 and AtbHLH39 in regulating iron uptake gene expression for iron homeostasis in *Arabidopsis*. *Cell Res.* **18**, 385–397 (2008).
13. N. Wang *et al*., Requirement and functional redundancy of Ib subgroup bHLH proteins for iron deficiency responses and uptake in *Arabidopsis thaliana*. *Mol. Plant* **6**, 503–513 (2013).
14. J. Zhang *et al*., The bHLH transcription factor bHLH104 interacts with IAA-LEUCINE RESISTANT3 and modulates iron homeostasis in *Arabidopsis*. *Plant Cell* **27**, 787–805 (2015).
15. X. Li, H. Zhang, Q. Ai, G. Liang, D. Yu, Two bHLH transcription factors, bHLH34 and bHLH104, regulate iron homeostasis in *Arabidopsis thaliana*. *Plant Physiol.* **170**, 2478–2493 (2016).
16. G. Liang, H. Zhang, X. Li, Q. Ai, D. Yu, bHLH transcription factor bHLH115 regulates iron homeostasis in *Arabidopsis thaliana*. *J. Exp. Bot.* **68**, 1743–1755 (2017).
17. F. Gao *et al*., The transcription factor bHLH121 interacts with bHLH105 (ILR3) and Its closest homologs to regulate iron homeostasis in *Arabidopsis*. *Plant Cell* **32**, 508–524 (2020).
18. R. Lei *et al*., bHLH121 functions as a direct link that facilitates the activation of FIT by bHLH IVc transcription factors for maintaining Fe homeostasis in *Arabidopsis*. *Mol. Plant* **13**, 634–649 (2020).
19. S. A. Kim, I. S. LaCroix, S. A. Gerber, M. L. Guerinot, The iron deficiency response in *Arabidopsis thaliana* requires the phosphorylated transcription factor URI. *Proc. Natl. Acad. Sci. U.S.A.* **116**, 24933–24942 (2019).
20. T. A. Long *et al*., The bHLH transcription factor POPEYE regulates response to iron deficiency in Arabidopsis roots. *Plant Cell* **22**, 2219–2236 (2010).
21. N. Tissot, *et al*., Transcriptional integration of the responses to iron availability in Arabidopsis by the bHLH factor ILR3. *New Phytol.* **223**, 1433–1446 (2019).
22. D. Selote, R. Samira, A. Matthiadis, J. W. Gillikin, T. A. Long, Iron-binding E3 ligase mediates iron response in plants by targeting basic helix-loop-helix transcription factors. *Plant Physiol.* **167**, 273–286 (2015).
23. M. N. Hindt *et al*., BRUTUS and its paralogs, BTS LIKE1 and BTS LIKE2, encode important negative regulators of the iron deficiency response in *Arabidopsis thaliana*. *Metallomics* **9**, 876–890 (2017).
24. M. Li *et al*., The iron deficiency response regulators IAA-LEUCINE RESISTANT3 and bHLH104 possess different targets and have distinct effects on photosynthesis in Arabidopsis. *J. Plant Biol.* **62**, 109–119 (2019).
25. H.-Y. Wang *et al*., Iron deficiency-mediated stress regulation of four subgroup Ib BHLH genes in *Arabidopsis thaliana*. *Planta* **226**, 897–908 (2007).
26. A. B. Sivitz, V. Hermand, C. Curie, G. Vert, *Arabidopsis* bHLH100 and bHLH101 control iron homeostasis via a FIT-independent pathway. *PLoS One* **7**, e44843 (2012).
27. N. Msilini *et al*., Inhibition of photosynthetic oxygen evolution and electron transfer from the quinone acceptor QA- to QB by iron deficiency. *Photosynth. Res.* **107**, 247–256 (2011).
28. N. Msilini *et al*., How does iron deficiency disrupt the electron flow in photosystem I of lettuce leaves? *J. Plant Physiol.* **170**, 1400–1406 (2013).
29. F. Morales, R. Belkhodja, A. Abadía, J. Abadía, Photosystem II efficiency and mechanisms of energy dissipation in iron-deficient, field-grown pear trees (*Pyrus communis* L.). *Photosynth. Res.* **63**, 9–21 (2000).
30. J. L. Moseley *et al*., Adaptation to Fe-deficiency requires remodeling of the photosynthetic apparatus. *EMBO J.* **21**, 6709–6720 (2002).
31. A. Saito, T. Iino, K. Sonoike, E. Miwa, K. Higuchi, Remodeling of the major light-harvesting antenna protein of PSII protects the young leaves of barley (*Hordeum vulgare* L.) from photoinhibition under prolonged iron deficiency. *Plant Cell Physiol.* **51**, 2013–2030 (2010).
32. A. Saito *et al*., Fe deficiency induces phosphorylation and translocation of Lhcb1 in barley thylakoid membranes. *FEBS Lett.* **588**, 2042–2048 (2014).
33. Y. Wang *et al*., Fe deficiency induced changes in rice (*Oryza sativa* L.) thylakoids. *Environ. Sci. Pollut. Res. Int.* **24**, 1380–1388 (2017).
34. D. Eide, M. Broderius, J. Fett, M. L. Guerinot, A novel iron-regulated metal transporter from plants identified by functional expression in yeast. *Proc. Natl. Acad. Sci. U.S.A.* **93**, 5624–5628 (1996).
35. N. J. Robinson, C. M. Procter, E. L. Connolly, M. L. Guerinot, A ferric-chelate reductase for iron uptake from soils. *Nature* **397**, 694–697 (1999).
36. L. Dall'Osto, S. Cazzaniga, H. North, A. Marion-Poll, R. Bassi, The *Arabidopsis aba4-1* mutant reveals a specific function for neoxanthin in protection against photooxidative stress. *Plant Cell* **19**, 1048–1064 (2007).
37. C. Triantaphylidès, M. Havaux, Singlet oxygen in plants: Production, detoxification and signaling. *Trends Plant Sci.* **14**, 219–228 (2009).
38. F. Ramel *et al*., Light-induced acclimation of the *Arabidopsis chlorina1* mutant to singlet oxygen. *Plant Cell* **25**, 1445–1462 (2013).
39. E. Koh, R. Carmieli, A. Mor, R. Fluhr, Singlet oxygen induced membrane disruption and serpin-protease balance in vacuolar driven cell death in *Arabidopsis thaliana*. *Plant Physiol.* **171**, 1616–1625 (2016).
40. R. Nakano, H. Ishida, A. Makino, T. Mae, In vivo fragmentation of the large subunit of ribulose-1,5-bisphosphate carboxylase by reactive oxygen species in an intact leaf of cucumber under chilling-light conditions. *Plant Cell Physiol.* **47**, 270–276 (2006).
41. A. M. Timperio, G. M. D'Amici, C. Barta, F. Loreto, L. Zolla, Proteomics, pigment composition, and organization of thylakoid membranes in iron-deficient spinach leaves. *J. Exp. Bot.* **58**, 3695–3710 (2007).
42. M. Khatoon *et al*., Quality control of photosystem II: Thylakoid unstacking is necessary to avoid further damage to the D1 protein and to facilitate D1 degradation under light stress in spinach thylakoids. *J. Biol. Chem.* **284**, 25343–25352 (2009).
43. M. Herbstová, S. Tietz, C. Kinzel, M. V. Turkina, H. Kirchhoff, Architectural switch in plant photosynthetic membranes induced by light stress. *Proc. Natl. Acad. Sci. U.S.A.* **109**, 20130–20135 (2012).
44. M. Pribil, M. Labs, D. Leister, Structure and dynamics of thylakoids in land plants. *J. Exp. Bot.* **65**, 1955–1972 (2014).
45. T. Schumann, S. Paul, M. Melzer, P. Dörmann, P. Jahns, Plant growth under natural light conditions provides highly flexible short-term acclimation properties toward high light stress. *Front Plant Sci* **8**, 681 (2017).
46. S. Järvi, M. Suorsa, E.-M. Aro, Photosystem II repair in plant chloroplasts—Regulation, assisting proteins and shared components with photosystem II biogenesis. *Biochim. Biophys. Acta BBA - Bioenerg.* **1847**, 900–909 (2015).
47. J. P. Dekker, E. J. Boekema, Supramolecular organization of thylakoid membrane proteins in green plants. *Biochim. Biophys. Acta BBA - Bioenerg.* **1706**, 12–39 (2005).
48. G. Sandmann, Consequences of iron deficiency on photosynthetic and respiratory electron transport in blue-green algae. *Photosynth. Res.* **6**, 261–271 (1985).
49. J. A. Guikema, L. A. Sherman, Influence of iron deprivation on the membrane composition of *Anacystis nidulans*. *Plant Physiol.* **74**, 90–95 (1984).
50. J. C. Pushnik, G. W. Miller, Iron regulation of chloroplast photosynthetic function: Mediation of PS I development. *J. Plant Nutr.* **12**, 407–421 (1989).
51. J. J. Pierella Karlusich, N. Carrillo, Evolution of the acceptor side of photosystem I: Ferredoxin, flavodoxin, and ferredoxin-NADP$^+$ oxidoreductase. *Photosynth. Res.* **134**, 235–250 (2017).
52. M. Roncel *et al*., Iron deficiency induces a partial inhibition of the photosynthetic electron transport and a high sensitivity to light in the diatom *Phaeodactylum tricornutum*. *Front Plant Sci* **7**, 1050 (2016).
53. F. Müh, A. Zouni, The nonheme iron in photosystem II. *Photosynth. Res.* **116**, 295–314 (2013).
54. A. Krieger-Liszkay, C. Fufezan, A. Trebst, Singlet oxygen production in photosystem II and related protection mechanism. *Photosynth. Res.* **98**, 551–564 (2008).
55. B. Bossmann, J. Knoetzel, S. Jansson, Screening of chlorina mutants of barley (*Hordeum vulgare* L.) with antibodies against light-harvesting proteins of PS I and PS II: Absence of specific antenna proteins. *Photosynth. Res.* **52**, 127–136 (1997).
56. D. Shinozaki *et al*., Autophagy increases zinc bioavailability to avoid light-mediated reactive oxygen species production under zinc deficiency. *Plant Physiol.* **182**, 1284–1296 (2020).
57. C. Fufezan, A. W. Rutherford, A. Krieger-Liszkay, Singlet oxygen production in herbicide-treated photosystem II. *FEBS Lett.* **532**, 407–410 (2002).
58. M. Huysmans, S. Lema A, N. S. Coll, M. K. Nowack, Dying two deaths—Programmed cell death regulation in development and disease. *Curr. Opin. Plant Biol.* **35**, 37–44 (2017).
59. R. Samira *et al*., The bHLH transcription factor ILR3 modulates multiple stress responses in *Arabidopsis*. *Plant Mol. Biol.* **97**, 297–309 (2018).
60. B. Li *et al*., Promoter-based integration in plant defense regulation. *Plant Physiol.* **166**, 1803–1820 (2014).
61. M. D. Page *et al*., Fe sparing and Fe recycling contribute to increased superoxide dismutase capacity in iron-starved *Chlamydomonas reinhardtii*. *Plant Cell* **24**, 2649–2665 (2012).
62. B. Andersson, J. M. Anderson, Lateral heterogeneity in the distribution of chlorophyll-protein complexes of the thylakoid membranes of spinach chloroplasts. *Biochim. Biophys. Acta BBA - Bioenerg.* **593**, 427–440 (1980).
63. R. Nevo, D. Charuvi, O. Tsabari, Z. Reich, Composition, architecture and dynamics of the photosynthetic apparatus in higher plants. *Plant J.* **70**, 157–176 (2012).
64. R. Fristedt *et al*., Phosphorylation of photosystem II controls functional macroscopic folding of photosynthetic membranes in *Arabidopsis*. *Plant Cell* **21**, 3950–3964 (2009).
65. J. Rodríguez-Celma *et al*., The transcriptional response of *Arabidopsis* leaves to Fe deficiency. *Front Plant Sci* **4**, 276 (2013).
66. W. H. J. Wood *et al*., Dynamic thylakoid stacking regulates the balance between linear and cyclic photosynthetic electron transfer. *Nat. Plants* **4**, 116–127 (2018).
67. Y. Munekage *et al*., Cyclic electron flow around photosystem I is essential for photosynthesis. *Nature* **429**, 579–582 (2004).
68. A. P. Hertle *et al*., PGRL1 is the elusive ferredoxin-plastoquinone reductase in photosynthetic cyclic electron flow. *Mol. Cell* **49**, 511–523 (2013).
69. M. Pribil *et al*., Fine-tuning of photosynthesis requires CURVATURE THYLAKOID1-mediated thylakoid plasticity. *Plant Physiol.* **176**, 2351–2364 (2018).
70. Z.-Y. Du *et al*., Galactoglycerolipid lipase PGD1 Is involved in thylakoid membrane remodeling in response to adverse environmental conditions in chlamydomonas. *Plant Cell* **30**, 447–465 (2018).
71. E. Devadasu *et al*., Changes in the photosynthetic apparatus and lipid droplet formation in *Chlamydomonas reinhardtii* under iron deficiency. *Photosynth. Res.* **139**, 253–266 (2019).
72. M. Suorsa, *et al*., Dark-adapted spinach thylakoid protein heterogeneity offers insights into the photosystem II repair cycle. *Biochim. Biophys. Acta BBA - Bioenerg.* **1837**, 1463–1471 (2014).
73. R. A. Rampey *et al*., An *Arabidopsis* basic helix-loop-helix leucine zipper protein modulates metal homeostasis and auxin conjugate responsiveness. *Genetics* **174**, 1841–1857 (2006).